Chapter 4

Mechanistic and Spectroscopic study for adsorption of Cr^{6+} and Cr^{3+} onto the adsorbents prepared from Palm Shell Powder

Outline:

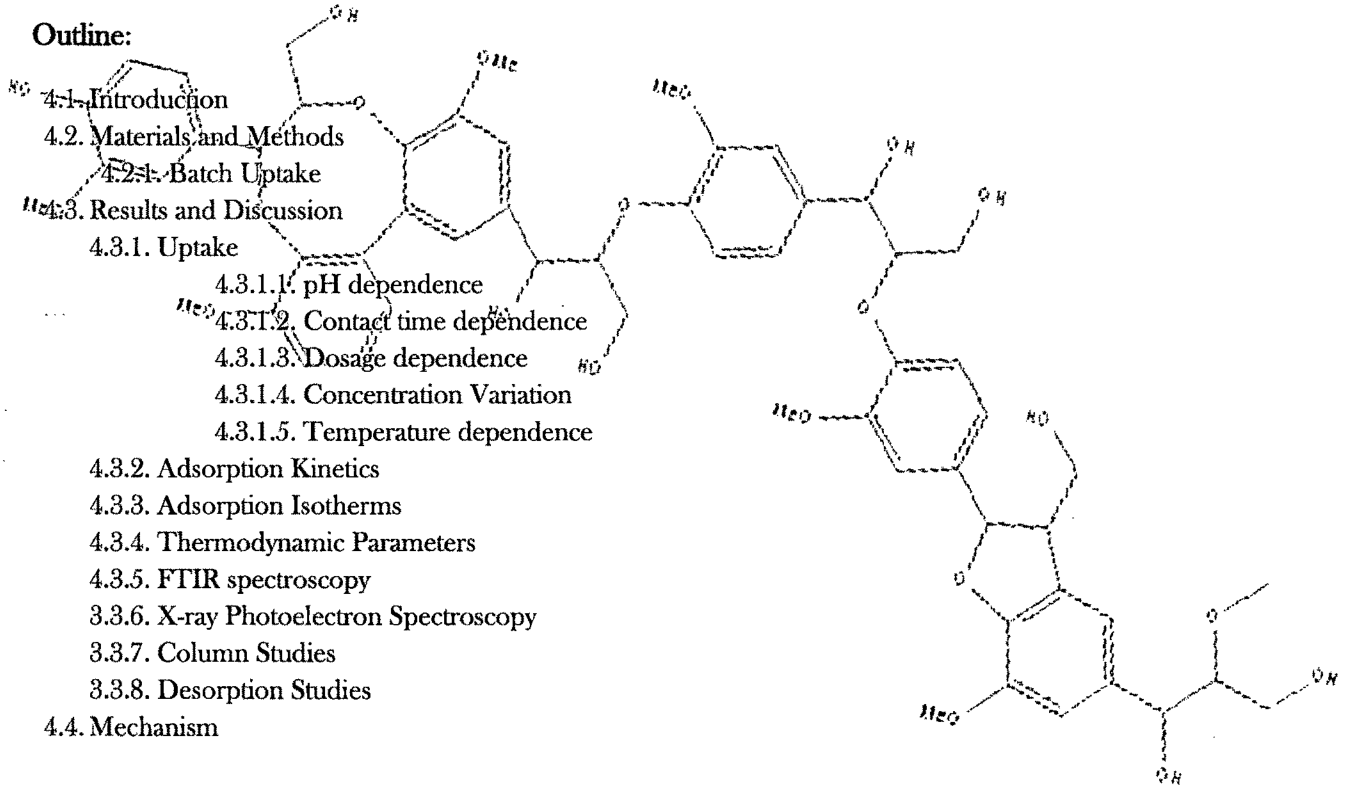

4.1. Introduction

Among the several oxidation states(di-, tri-, penta- and hexa-) of chromium, trivalent chromium together with the hexavalent state can be mainly present in the aquaticenvironment [1]. Although trivalent chromium is less toxic than hexavalent chromium, a long-term exposure to trivalent chromium is known to cause allergic skin reactions and cancer [2]. As a result, the total chromium level in the effluent is strictly regulated in many countries.Hexavalent chromium species are strong oxidants that act as carcinogens, mutagens, and teratogens in biologicalsystems. Hexavalent chromium exists in water as oxyanions such as chromate ($HCrO_4^-$) and dichromate ($Cr_2O_7^{2-}$). Itsspeciation is dependent on the pH. It causes diseases such as epigastric pain nausea, vomiting, severe diarrhea, andhemorrhage by ingestion. The maximum allowed contaminant drinking level for the drinking water is 0.05 mg/L [3].

Several inexpensive sorbents have been tested in the removal of hexavalent chromium as given in Table1.3 of chapter 1. Most reports claim that the Cr^{6+} was removed from aqueous systems by anionic adsorption [4-24]but it has been newly explained that these findings were misinterpreted due to errors in measuring chromium species in aqueous phase, insufficient contact time required for equilibrium, and the lack of information about the oxidation state of the chromium bound on the biomaterials [25].Someresearchers have reported that the removal of $Cr^{6+}$was partly through reduction, as well as anionic adsorption,and the partial reduction could take place only under stronglyacidic conditions ($pH < 2.5$) [26-31].

Therefore the aim of this study is to i) determine the influence of the various parameters on the adsorption of hexavalent and trivalent Cr, ii) Evaluation of the adsorption capacity of the adsorbents by studying the equilibriumadsorption isotherms of Cr^{6+}.iii) Fitthe equilibrium data to five different isotherm models,and obtain the values of parameters of the isotherms. iv) Obtain breakthrough curves using column adsorptionand fit the data to various column models and v) Use XPS and FT-IR spectroscopic techniques to gain insight into the mechanism of adsorption of hexavalent chromium onto the adsorbents under study.

4.2.Material and Methods.

4.2.1. Batch Uptake.

A stock solutions of Cr^{3+} and Cr^{6+} were prepared by dissolving 5.13 and 2.83 g of $CrCl_3.6H_2O$and $K_2Cr_2O_7$(E-Merck) respectively in slightly acidified double distilled water and making upto 1L to give 1000 mg/L of Cr^{3+} and Cr^{6+}solutions. Working standards were prepared by diluting different volumes of the stock solution to obtain the desired concentration. Batch adsorption experiments were conducted as discussed in Chapter 3.

At the end of the predetermined time intervals, the suspensions were filtered and the filterate was analysed to find the uptake of chromium by the adsorbents under study. The Cr^{6+}concentration in the filterate was analysed spectrophotometrically by UV spectrophotometer (Elico SL177) at 540 nm after using diphenylcarbazide complexing agent, while the total chromium concentration was determined by ICP analysis (ICP-AES, Thermo Jarrel Ash, Model Trace Scan). The Cr(III) concentration was obtained from the differencebetween the total Cr and Cr(VI) concentrations in the filterate.

4.3.Results and Discussion

4.3.1. Uptake studies.

4.3.1.1. *pH dependence.*

The pH of the medium from which adsorption is taking place is an important controlling parameter in heavy metal adsorption process. Its effect on the removal of Cr^{6+}/ Cr^{3+}ion (initial concentration 100ppm) was studied by varying pH from 1 to10.

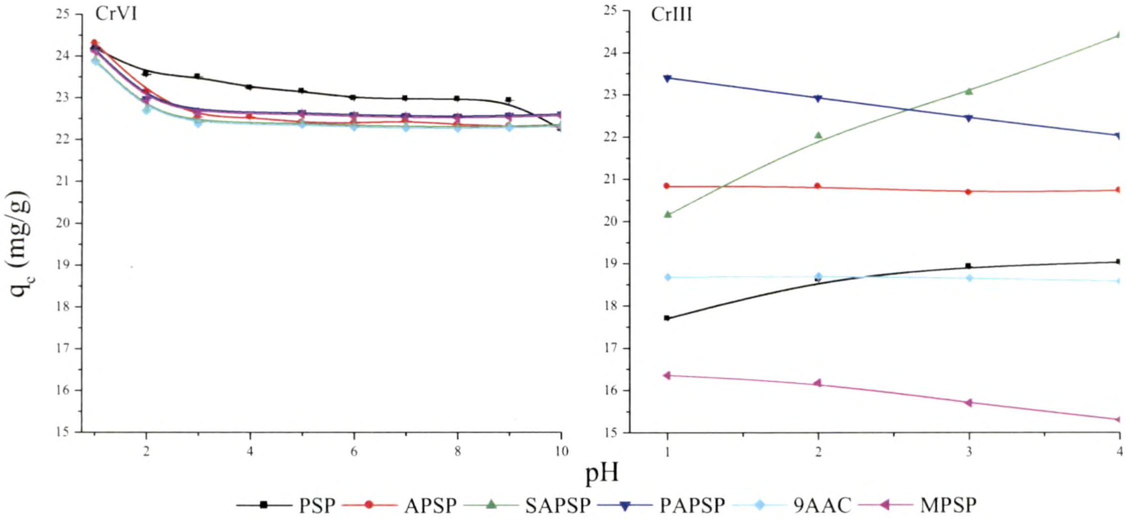

Operating parameters: 180 rpm,100ppm of Cr^{6+}/ Cr^{3+}, 0.1g adsorbent, time 240 min, temperature 30 ^{0}C, pH 1-4

Figure 4.1.Effect of pH, time, dose, initial concentration of Cr^{6+}/ Cr^{3+}

Cr^{3+} predominates at pH<3.0 whereas at pH>3.5, hydrolysis of aqueous Cr^{3+} yields trivalentchromium hydroxy species [$CrOH^{2+}$, $Cr(OH)_2^+$, $Cr(OH)_3$and $Cr(OH)_4^-$] [32]. Hexavalent chromiumexists primarily as salts of chromic acid (H_2CrO_4), hydrogenchromate ion ($HCrO_4^-$) and chromate ion (CrO_4^{2-}),depending on the pH. H_2CrO_4 predominates at pH's less than about 1.0, $HCrO_4^-$at pH's between 1.0 and 6.0, and CrO_4^{2-}at pHs above about 6[33].

Figure 4.1 shows that for all the adsorbents under study adsorption of Cr^{6+} ionwas maximum at ~pH 1, decreased slightly till pH 3 and then remainedconstant for the remaining range of pH studied. In the case of Cr^{3+}maximum adsorption was observed at pH 1 with slight decrease in adsorption till pH4 observed for APSP, PAPSP and MPSP. On the other hand for PSP and 9AAC a slight increase in Cr^{3+}adsorption was observed as pH was increased from 1 to 4,whilethe increase in adsorption was found to be significant for SAPSP.Similar reports of optimum adsorption at pH 4 for trivalent chromium are available in literature[34].

At low pH conditions, the amino ($-NH_2$) phenolic and carboxyl groups may become protonated, thus making the biomass more positively charged resulting in electrostatic attraction of the Cr^{6+} species.The acid chromate ion species ($HCrO_4^-$) is reported to be the major form of Cr^{6+} at this range of pH value of 1-4[35, 36].The phenolic groups, carboxyl and amino groups may contribute to Cr^{3+} binding at low pH which may be attributed to competition of chromium (III) species with H^+ or H_3O^+ ions for the surface functional groups as evidenced by considerable adsorption of Cr^{3+} at low pH in the case of APSP,PAPSP and MPSP and maximum adsorption in the case of SAPSP,PSP and 9AAC. As pH increases from 1 to 4, deprotonation of these functional groups leads to a slightly increasednegative charge on the biomass resulting in repulsionof anionic Cr^{6+} species, while positively charged Cr^{3+} experiences increasedattraction to the biomass.At higher pH values (>4.0) formation of chromium hydroxide starts, resulting in reduced adsorption.

4.3.1.2. *Contact time dependence.*

Contact time variation shows that equilibrium is achieved faster (80 min) when SAPSP & 9AAC was used as the adsorbent as compared to other adsorbents under study (PSP, SAPSP, PAPSP and MPSP) where equilibrium was achieved in 150 min (Figure 4.2) in case of Cr^{6+} whereas all the adsorbents showed similar trend for Cr^{3+} adsorption and equilibrium was achieved in 120 min.

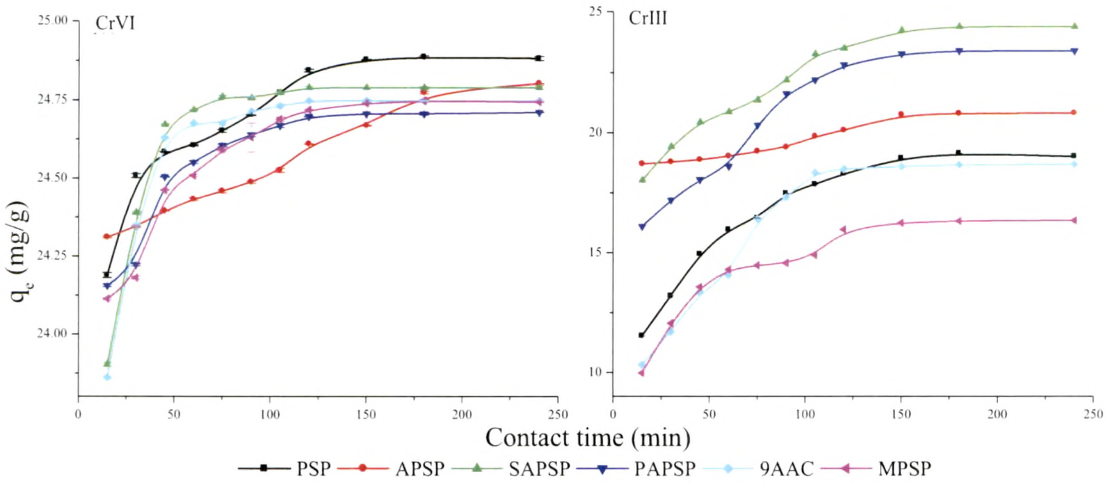

Operating parameters: 180 rpm,100ppm of Cr^{6+}/ Cr^{3+}, 0.1g adsorbent, time 15-240 min, temperature 30 ^{0}C, pH 1

Figure 4.2.Effect of contact time of Cr^{6+}/ Cr^{3+}

The rate of adsorption is very fast initially with about >95% of Cr^{6+} being removed within few minutes followed by a decreased rate with the approach of equilibrium when compared with slow rate of adsorption of Cr^{3+} with 40-90% in 120 min. The removal rate is high initially due to the presence of free binding sites which gradually become saturated with time resulting in decreased rate of adsorption as equilibrium approaches. This indicates that the adsorption is mainly through surface binding. Similar observations were made by Das et al [37].

4.3.1.3. *Dosagedependence.*

The effect of dose of adsorbents under study on the removal of Chromium [Cr^{6+}& Cr^{3+}] is shown in Figure 4.3, which illustrates the adsorption of Chromium ion with change of the adsorbent dose from 0.02 to 0.12g.

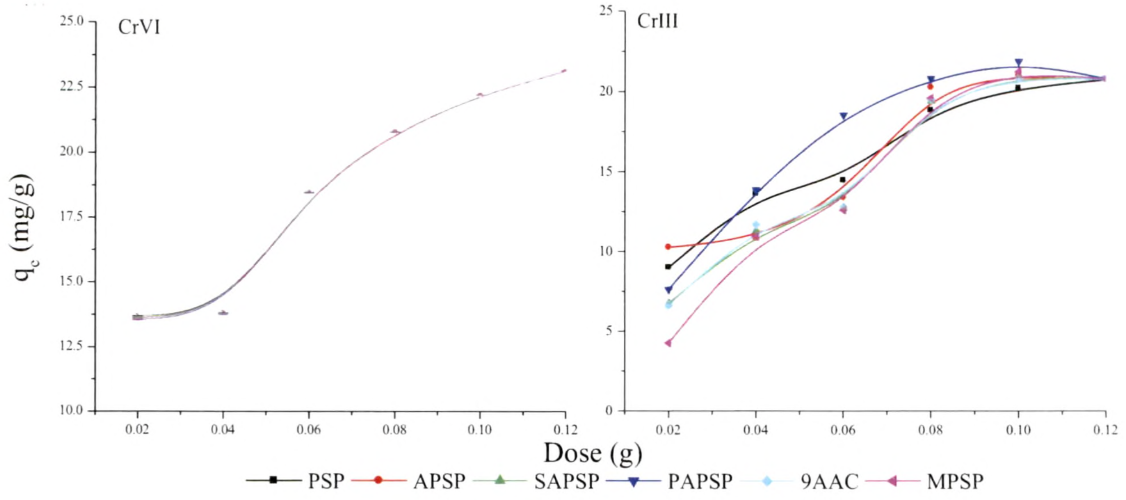

Operating parameters: 180 rpm,100 ppm of Cr^{6+}/ Cr^{3+}, time 240 min, temperature 30 ^{0}C, pH 1

Figure 4.3.Effect of initial concentration of Cr^{6+}/ Cr^{3+}

As inferred from Figure4.3, for a fixed metal initial concentration, increasing the adsorbent dose provided greater surface area and availability of more active sites [38], thus leading to the enhancement of metal ion uptake for both Cr^{6+} and Cr^{3+}.

4.3.1.4. *Concentration Variation.*

Variation in initial concentration of Cr^{6+}/ Cr^{3+}as shown in Figure 4.4 showed similar trend. In case of Cr^{6+} maximum adsorption capacity was found to be higher than for Cr^{3+}.

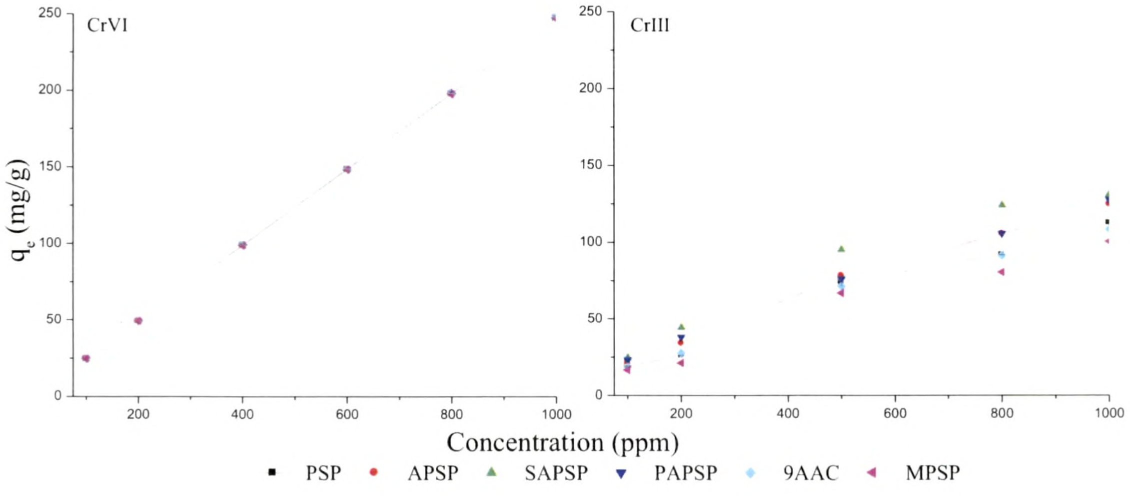

Operating parameters: 180 rpm,0.1g adsorbent, time 240 min, temperature 30 ^{0}C, pH 1

Figure 4.4.Effect of initial concentration of Cr^{6+}/ Cr^{3+}

4.3.1.5. *Temperature variation.*

Temperature studies showed (Figure 4.5) almost the same trend for all the adsorbents under study. From the figure it can be seen that uptake decreases as temperature increases indicating that the mechanism of adsorption is exothermic in nature for both Cr^{6+}/ Cr^{3+}.

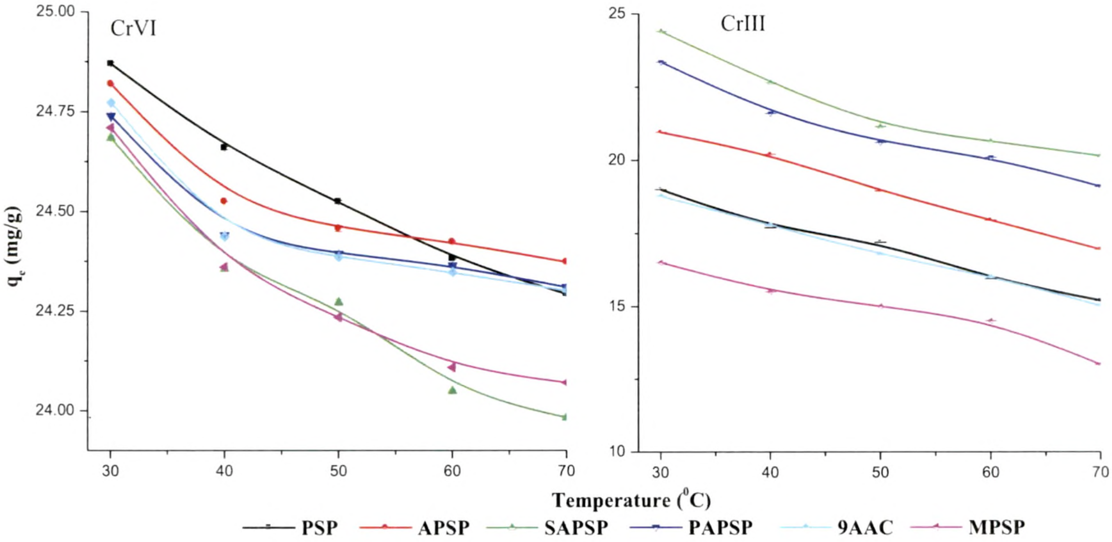

Operating parameters: 180 rpm,1000 ppm of Cr^{6+}/ Cr^{3+}, 0.1g adsorbent, time 240 min, pH 1

Figure 4.5. Effect of temperature on uptake of Cr^{6+}/ Cr^{3+} ions by PSP, MPSP, APSP, SAPSP, PAPSP and 9AAC

4.3.2. Adsorption Kinetics.

Adsorption of Cr^{6+}/Cr^{3+} ions onto PSP, APSP, SAPSP, PAPSP, 9AAC and MPSP was carried out for 240 min to ensure complete attainment of equilibrium. The kinetic models of Pseudo First order, Pseudo Second order, Intraparticle diffusion, Bangham, Elovich and Liquid film diffusion models were studied and the kinetic constants for the adsorption of chromium by all the adsorbents under study are presented in Table 4.1.

Table 4.1. Kinetic parameters

Cr^{6+}/ Cr^{3+}	PSP	APSP	SAPSP	PAPSP	9AAC	MPSP
qe (exp)	24.87/ 19.00	24.82/ 20.95	24.68/ 24.40	24.74/ 23.35	24.77/ 18.78	24.71/ 16.50
Pseudo 2ndorder						
$q_e(mg.g^{-1})$	24.630/ 18.195	24.845/ 21.263	24.771/ 21.061	24.808/ 25.006	62.112/ 16.667	24.857/ 17.343
K_2 (g.mgmin^{-1})	0.058/ 0.054	0.104/ 0.008	0.082/ 0.005	0.099/ 0.003	0.012/ 0.004	0.042/ 0.004
r^2	1.000/ 0.999	1.000/0.999	1.000/ 0.99	1.000/ 0.999	0.999/ 0.995	0.999/ 0.99
SD	0.007/ 0.013	0.005/ 0.010	0.004/ 0.014	0.005/ 0.015	0.001/ 0.018	0.015/ 0.015
Lagergren						
$q_e(mg.g^{-1})$	0.754/ 5.879	1.219/ 7.262	0.927/ 10.385	1.219/ 18.892	1.064/ 8.404	1.833/ 15.354
K_1 (min^{-1})	-0.016/ -0.022	-0.043/ -0.026	-0.029/ -0.025	-0.041/ -0.029	-0.027/ -0.34	-0.006/ -0.032
r^2	0.966/ 0.934	0.969/ 0.896	0.991/ 0.941	0.975/ 0.958	0.986/ 0.934	0.997/ 0.955
SD	0.068/ 0.025	0.167/ 0.032	0.062/ 0.087	0.144/ 0.078	0.067/ 0.082	0.007/ 0.041
Intra Particle Diffusion						
K_{ip}(mg/g/min)	0.041/ 0.342	0.012/ 0.230	0.024/ 0.449	0.013/ 0.739	0.034/ 0.874	0.052/ 0.527
r^2	0.927/ 0.847	0.821/ 0.954	0.889/ 0.960	0.859/ 0.946	0.898/ 0.929	0.982/ 0.920
SD	0.049/ 0.087	0.024/ 0.066	0.037/ 0.074	0.023/ 0.092	0.050/ 0.076	0.030/ 0.087
Elovich						
β (g.mg^{-1})	3.983/ 0.637	3.478/ 1.074	4.429/ 0.521	3.475/ 0.312	3.788/ 0.260	5.273/ 0.421
α (mg.g^{-1}min^{-1})	2.562E+93/ 1896285.996	6.800E+80/ 5.368E+16	5.934E+103/ 305002.297	3.945E+80/ 388.126	1.218E+88/ 2.000	1.89E+124/ 124.328
r^2	0.972/ 0.913	0.859/ 0.906	0.941/ 0.963	0.865/ 0.964	0.959/ 0.959	0.933/ 0.977
SD	0.051/ 0.063	0.047/ 0.073	0.069/ 0.056	0.143/ 0.076	0.066/ 0.097	0.062/ 0.044
Liquid film diffusion model						
K_{FD}	0.029/ -0.022	0.043/ -0.026	0.038/ -0.025	0.029/ -0.029	0.036/ -0.033	0.025/ -0.032
r^2	0.892/ 0.934	0.905/ 0.895	0.981/ 0.940	0.904/ 0.958	0.969/ 0.934	0.886/ 0.955
SD	0.074/ 0.073	0.082/ 0.073	0.050/ 0.042	0.094/ 0.041	0.041/ 0.051	0.090/ 0.055
Bangham						
K_{BM}	-113.37/ -126.10	-113.39/ -120.38	-113.46/ -123.75	-113.44/ -122.31	-113.72/ -132.28	-113.72/ -131.44
α	4.660E-05/ 4.41E-04	4.46E-05/ 2.60E-04	3.98E-05/ 5.26E-04	4.51E-05/ 7.70E-04	4.80E-05/ 0.001	4.29E-05/ 7.84E-04
r^2	0.840/ 0.738	0.616/ 0.951	0.768/ 0.907	0.625/ 0.874	0.809/ 0.840	0.983/ 0.808
SD	0.002/ 0.028	0.004/ 0.006	0.002/ 0.017	0.004/ 0.020	0.003/ 0.057	0.001/ 0.040

The pseudo second order kinetics provided the best fit for the kinetic data at optimumpH. The q_e values were very close to the experimental q_e value and correlation coefficient values were 0.995-1.00 for PSP, APSP, SAPSP, PAPSP, 9AAC and MPSP for both Cr^{3+} and Cr^{6+}. This suggests that the rate limiting step in adsorption of chromium is chemisorption involving valence forces through the exchange of electrons between sorbent and sorbate[39, 40], complexation, coordination and/ or chelation.

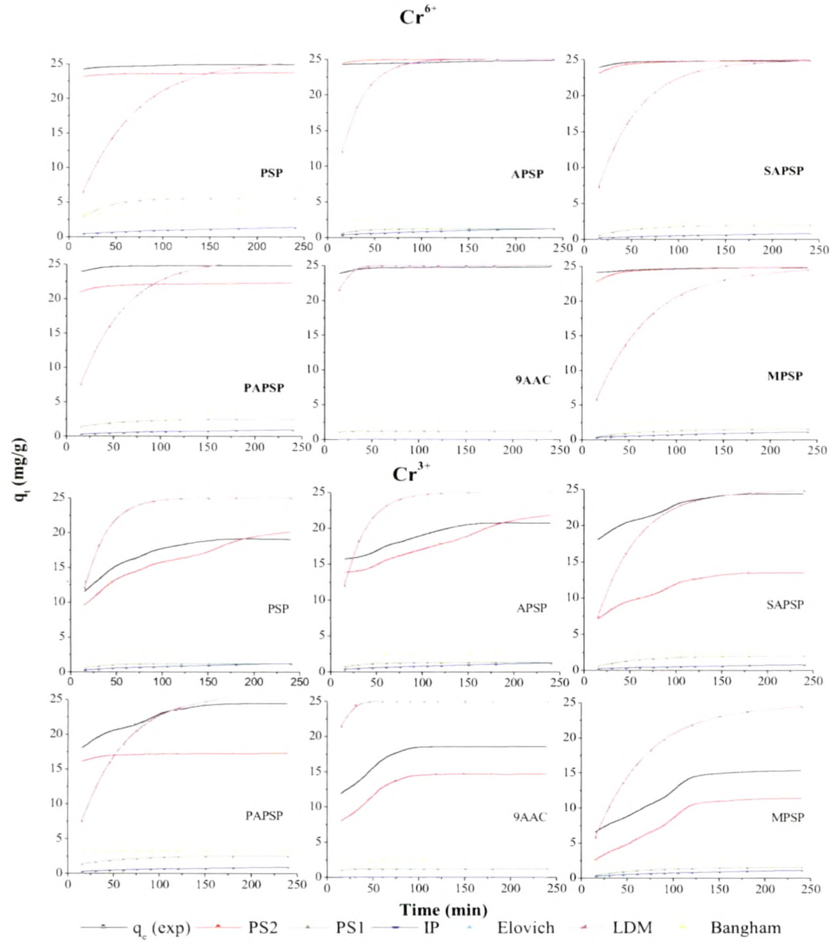

Operating parameters: 180 rpm,100ppm of Cr^{6+}/ Cr^{3+}, 0.1g adsorbent, time 15-240 min, temperature 30 ^{0}C, pH 1

Figure 4.6. Kinetics for Cr^{6+} and Cr^{3+} by PSP, APSP, SAPSP, PAPSP, 9AAC and MPSP

In pseudo first order model the $q_{e(exp)}$ values were much higher than q_e fitted values (Figure 4.6) for both Cr^{3+} and Cr^{6+}. The large discrepancies show that the reaction cannot be classified as pseudo first order although this plot has reasonably good correlation coefficient from the fitting process. This underestimate of the amount of binding sites is probably due to the fact that q_e was determined from the y-intercept (0, 1). This intercept is affected strongly by the short term metal uptake, which is much lower than equilibrium uptake [41]. This has been observed by several other workers [42-44]. This could be due to boundary layer controlling the beginning of the adsorption process [44]. Elovich model's correlation coefficients (0.859-0.977) provided a bad fit to the experimental data and hence we can not predict any meaningful information or any definite mechanism. The Liquid film diffusion model is applicable when flow of the adsorbate from the bulk liquid to the surface of the adsorbent determines the rate constant. The curves did not pass though origin as required by the model but very small intercepts indicates that diffusion of chromium from the liquid phase to the adsorbent surface might be having some role in deciding the rate processes. The Weber and Morris adsorption kinetic model was plotted using the equation given in Chapter 3 Table3.1.

The plots obtained for PSP, APSP, SAPSP, PAPSP, 9AAC and MPSP do not pass through origin implying that intraparticle diffusion is not the only operative mechanism.The intraparticle diffusion rate is fastest in PSP &APSP, the order being APSP~PSP>SAPSP>MPSP>PAPSP>9AAC for Cr^{3+};APSP~PAPSP>SAPSP>9AAC>PSP>MPSPfor Cr^{6+}as evident from intraparticle diffusion rate constants. Finally, in order to further confirm the occurrence of intraparticle diffusion, Bangham equation (Chapter 3 Table3.1) was applied to the adsorption data. The double logarithmic plots obtained with very less correlation coefficients (>0.616) for both Cr^{6+} and Cr^{3+}indicated very less contribution of pore diffusion towards adsorption process. The lowest r^2 value for 9AAC is in agreement with the results of intraparticle diffusion. The not so linear curves indicated the diffusion of adsorbate into pores of the sorbent is not the only rate controlling step.

Adsorption capacity of the adsorbents for Cr^{6+} washighest at pH 1, whereas Cr^{3+}adsorption was highest at pH4 which is consistent with results of others [45].Initial rapid uptake implies the binding of adsorbate ions on the surface of adsorbents under study throughproton exchange at optimum pH(pH 1) as Cr^{6+} occurs in its anionic form and preferably bind at pH1.Later on slower adsorption might be due to intraparticle diffusion, and diffusion of chromium from the aqueous phase to the adsorbent due to weak acidic and basic groups such as carboxyl, hydroxyl, amino groups at pH >1.

4.3.3. Adsorption Isotherms.

For modeling ofchromiumuptake Freundlich, Langmuir, Temkin, Dubinin-Radushkevich (DR), Flory-Huggins, Elovich and Halsey isotherm models were employed. Adsorption isotherms of the type $q_e$vsC_e were also used to verify the isotherm models. The values of model constants along with their correlation coefficients, r^2 and SD values for all the systems studied are presented in Table 4.2.

Table 4.2. Isotherms parameters for different adsorbents Cr^{6+}/ Cr^{3+}

Cr^{6+}/ Cr^{3+}	PSP	APSP	SAPSP	PAPSP	9AAC	MPSP
Freundlich						
$q_{e(exp)}$ (mg/g)	24.87/ 19.00	24.82/ 20.95	24.68/ 24.40	24.74/ 23.35	24.77/ 18.78	24.71/ 16.50
K_F(mg.g^{-1})(dm^3/mg)$^{1/n}$	5.08/ 1.47	3.66/ 1.13	4.36/ 1.88	3.54/ 3.45	3.84/ 2.71	4.31/ 1.49
n	1.37/ 1.00	1.00/ 1.49	1.07/ 1.85	0.96/ 2.98	0.93/ 2.53	1.01/ 1.69
r^2	0.997/ 0.959	0.995/ 0.948	0.991/ 0.989	0.999/ 0.993	0.996/ 0.985	0.995/ 0.976
SD	0.038/ 0.013	0.044/ 0.031	0.056/ 0.054	0.034/ 0.044	0.038/ 0.062	0.046/ 0.083
Langmuir						
K_L (dm^3.mg^{-1})	0.164/ 0.006	0.071/ 0.004	0.075/ 0.008	0.051/ 0.034	0.073/ 0.012	0.107/ 0.006
q_m (mg.g^{-1})	289/ 138	303/ 133	284/ 149	313/ 137	262/ 136	249/ 154
ΔG (kJ.mol^{-1})	-4.71/ -13.32	-6.88/ -14.31	-6.72/ 12.67	-7.73/ -8.79	-6.79/ -11.49	-5.79/ -13.41
r^2	0.993/ 0.985	0.910/ 0.981	0.987/ 0.984	0.994/ 0.996	0.998/ 0.960	0.983/ 0.991
SD	0.002/ 0.054	0.002/ 0.046	0.001/ 0.030	0.006/ 0.057	0.003/ 0.005	0.002/ 0.088
Temkin						
-ΔH (kJ.mol^{-1})	7.346/ 7.633	10.443/ 7.670	10.357/ 8.726	10.983/ 11.741	9.755/ 9.418	8.975/ 9.292
K_T (dm^3.mg^{-1})	0.319/ 0.146	0.333/ 0.072	0.440/ 0.227	0.324/ 0.213	0.391/ 0.22	0.468/ 0.115
r^2	0.995/ 0.995	0.988/ 0.993	0.960/ 0.956	0.982/ 0.963	0.973/ 0.961	0.953/ 0.939
SD	0.077/ 0.036	0.031/ 0.068	0.082/ 0.054	0.023/ 0.071	0.045/ 0.025	0.073/ 0.069
DR						
q_m (mg.g^{-1})	187/ 167	229/ 166	216/ 178	221/ 174	235/ 173	253/ 179
E^0 (KJ)	12.46/ 10.44	10.72/ 11.94	14.85/ 19.92	11.21/ 15.04	1.29/ 1.19	12.82/ 10.75
r^2	0.956/ 0.957	0.972/ 0.967	0.939/ 0.960	0.954/ 0.959	0.971/ 0.954	0.975/ 0.967
SD	0.014/ 0.092	0.072/ 0.093	0.051/ 0.074	0.021/ 0.077	0.075/ 0.051	0.062/ 0.050
Halsey						
K_H (mg.g^{-1})(dm^3/mg)$^{1/n}$	0.823/ 0.751	0.716/ 0.777	0.758/ 0.388	0.699/ 0.416	0.701/ 0.332	0.745/ 0.359
n_H	-0.27/ -0.95	-0.33/ -0.95	-0.29/ -1.03	-0.34/ -1.04	-0.32/ -1.11	-0.29/ -0.69
r^2	0.997/ 0.994	0.995/ 0.999	0.991/ 0.994	0.997/ 0.997	0.996/0.996	0.995/ 0.997
SD	0.087/ 0.090	0.101/ 0.046	0.093/ 0.079	0.078/ 0.032	0.088/ 0.052	0.071/ 0.028
Flory-Huggins						
K_{FH} (mg.g^{-1})(dm^3/mg)$^{1/n}$	1.026/ 1.174	1.040/ 3.871	1.034/ 1.426	1.043/ 1.374	1.042/ 1.384	1.039/ 1.143
N_{FH}	0.998/ 2.307	0.996/ 2.528	0.997/ 2.558	0.996/ 2.634	0.995/ 2.607	0.996/ 3.282
r^2	1.000/ 0.999	1.000/ 1.000	1.000/ 0.990	1.000/ 0.986	1.000/ 0.992	1.000/ 0.998
SD	0.001/ 0.025	0.001/ 0.002	0.001/ 0.099	0.001/ 0.060	0.001/ 0.072	0.001/ 0.087
Elovich						
q_m (mg.g^{-1})	52.01/ 1.29	21.57/ 1.52	21.98/ 1.81	16.45/ 1.74	20.29/ 0.63	18.73/ 0.89
K_E (dm^3.mg^{-1})	1.627/ 9.23E+125	2.113/ 8.96E+55	0.651/ 5.19E+89	1.462/ 7.44E+95	1.006/ 1.37E+236	1.008/ 7.89E+125

r^2	0.994/ 0.994	0.997/ 0.924	0.988/ 0.985	0.995/ 0.967	1.000/ 0.911	0.999/ 0.988
SD	0.043/ 0.046	0.006/ 0.068	0.015/ 0.071	0.012/ 0.089	0.001/ 0.019	0.003/ 0.084

The value of $n \approx 1$ for the Freundlich model indicates favorable adsorption for Cr^{6+} whereas in case of adsorption of Cr^{3+} only PSP was having $n \approx 1$ others were having higher n values. The parameters K_L (equilibrium sorption constant) and qmax were calculated from the intercept and slope of the plot of C_e/q_e versus $C_e$of Langmuir isotherm model. Based on the correlation coefficient r^2 and standard deviations for Langmuir it varied from 0.910-0.998 for Cr^{6+} and 0.960-0.996 for Cr^{3+} with very less SD values. Langmuir monolayer adsorption capacity was found in good agreement with the experimental adsorption capacities.Adsorption of Cr^{6+} was found to be 2 times higher than adsorption of Cr^{3+} according to Langmuir maximum adsorption capacities on all the adsorbents. The order of preference of adsorbents to metal ion was found to be PAPSP>APSP>SAPSP~PSP>9AAC>MPSP for Cr^{6+} and MPSP~SAPSP>PAPSP~APSP~PSP~9AAC for Cr^{3+}. The maximum adsorption capacities found with these adsorbents were found to be comparable with literature (Chapter 1 Table 1.3) and in some cases higher than reported ones.

The correlation coefficients of Temkin Model (0.953 to 0.995 for Cr^{6+} and 0.939 to 0.995 for Cr^{3+}) indicate a satisfactory fit of the model to the experimental data. The variation of adsorption energy, ΔQ (7.346, 10.443, 10.357, 10.983, 9.755 and 8.975 for PSP, APSP, SAPSP, PAPSP, 9AAC and MPSP respectively in the case of Cr^{6+} and 7.633, 7.670, 8.726, 11.741, 9.418 and 9.292 for PSP, APSP, SAPSP, PAPSP, 9AAC and MPSP respectively in the case of Cr^{3+} is positive for all the sorbents under study, which indicated the adsorption process to be exothermic.

The Dubinin–Radushkevich model is applied in the form of linear equation as given in Chapter 3 Table3.1. The adsorption energy values calculated for $Cr^{6+}$are (12.462,10.715, 14.850, 11.207, 1.286 and 12.820 $KJmol^{-1}$) and for Cr^{3+} (10.438, 11.939, 19.924, 15.044, 1.198 and 10.751$KJmol^{-1}$) on PSP, APSP, SAPSP, PAPSP, 9AAC and MPSP respectively. The magnitude of E is useful for estimating the mechanism of the sorption reaction. In case of $E < 8.0$ kJ/mol, physical forces may affect the sorption; for E in the range 8–16 kJ/mol, ion exchange is the working mechanism, while for $E>16$ kJ/mol sorption may be dominated by particle diffusion [44, 46].It is thus evident from D-R model that for 9AAC physisorption is the predominant mechanism, while for PSP, APSP, SAPSP, PAPSP and MPSP ion-exchange is the predominant mechanism.

Multilayer adsorption is generally discussed by the Halsey equation and is found to fit well with the experimental data having r^2 (> 0.991 and 0.994 for Cr^{6+}/ Cr^{3+}) [38] indicating that the mechanism may be multilayer sorption for adsorbents under study while the low values of K_H suggest that multilayer sorption might be playing only a small role.The Flory-Huggins model was used to assess the isotherm data. From the linear plots of log(θ/C_0) versus log(1–θ) for chromium adsorption on the adsorbents under study and the correlation coefficient values (r^2 =1.00), it is apparent that the model shows good fits for the adsorbent under study. However the negative values of n and low values of k_{FH} imply that the model cannot be used to describe the adsorption data.

4.3.4. Thermodynamic Parameters.

The thermodynamic parameters of the sorption process could be determined from the experimental data obtained at various temperatures using the equations:

$$\Delta G^0 = \Delta H^0 - T\Delta S^0$$

The values of ΔH°and ΔS°can be calculated from the slope and intercept of the plots of ΔG° against 1/T (Figure4.7).

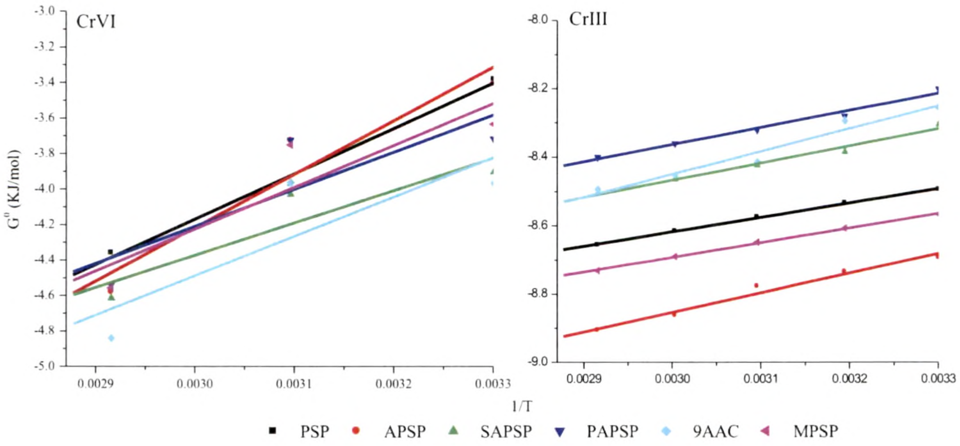

Operating parameters: 30-70 ^{0}C, 240 min, pH 1, 1000 ppm of Cr^{6+}/ Cr^{3+}, 0.1g adsorbent, 180 rpm.

Figure 4.7. Thermodynamic studies

Table 4.3. Thermodynamic Parameters for Chromium ions by PSP, APSP, SAPSP, PAPSP, 9AAC and MPSP

Cr^{3+}/ Cr^{6+}			
	ΔG (KJ/mol)	ΔS (KJ/molK)	ΔH (KJ/mol)
PSP	-28.439/ -48.113	0.082/ 0.094	-3.525/ -19.621
APSP	-31.425/ 58.613	0.088/ 0.110	-4.772/ -25.108
SAPSP	-29.323/ -39.861	0.083/ 0.081	-4.182/ -15.173
PAPSP	-29.029/ -43.819	0.082/ 0.087	-4.165/ -17.392
9AAC	-31.912/ -46.688	0.087/ 0.093	-5.562/ -18.473
MPSP	-28.708/ -48.121	0.083/ 0.094	-3.567/ -19.629

The negative value of ΔH° indicates that the adsorption of Cr^{6+}/ Cr^{3+} on PSP, APSP, SAPSP, PAPSP, 9AAC and MPSP is exothermic. Generally the absolute magnitude of the change in energy for physisorption is between (-20 and 0 KJ/mol); chemisorption has a range of (-400 and -80 KJ/mol). The negative value of ΔG° in Table 4.3 indicates that sorption of Cr^{6+}/ Cr^{3+}ion by PSP, APSP, SAPSP, PAPSP, 9AAC and MPSP to be physisorption and is spontaneous and thermodynamically favorable [47]. Also the ΔG° values become less negative with increase in temperature suggesting that adsorption is favored at lower temperatures and hence is exothermic. The positive values of ΔS° suggest increased randomness during adsorption and a high affinity of the adsorbent towards the adsorbate.

4.3.5. Fourier Transform Infrared Spectroscopy.

The absorption bands of FTIR spectra listed in Table 4.4reveal the changes in absorption bands of the surface functional groups of PSP, APSP, SAPSP, PAPSP, 9AAC and MPSP after chromium adsorption.

The metal loaded adsorbents showed a shift in the absorption frequencies of OH group indicating the binding of chromium to the –OH groups present in the adsorbents. The intensitiesof the peaks at ~1430, ~1250, ~893 and ~840cm^{-1} decreased whilethose at 1635 and 1556cm^{-1} increased. The peaks at 1430 and1250cm^{-1} were attributed to the $C–O–CH_3$ (methoxyl) deformationand C–OH (hydroxyl) bending of phenolic structure in lignin and those at 893 and 840 cm^{-1} were assigned to the out-of-plane CH bending vibrations of lignin (Table 4.4) [48-50]. The decreases in the intensities of these peaks indicated the oxidation of lignin in the adsorbents under study upon Cr^{6+} reaction.

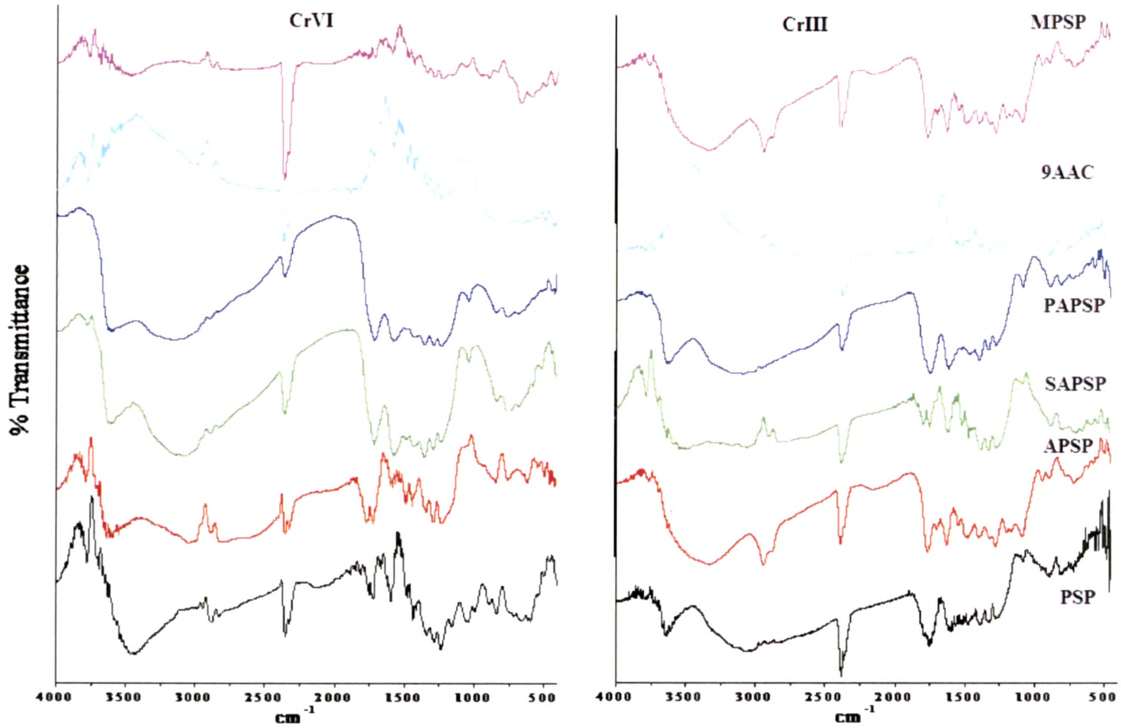

Figure 4.8. FTIR spectra for Cr^{6+} and Cr^{3+} loaded adsorbents

According to Elovitz and Fish[51]the oxidation of phenols leads to the formation of quinones containing carbonyl groups. Further oxidation of quinones may lead to the formation of carboxylate anions [52]. Thus, upon Cr^{6+} reaction, the increasing intensities at 1700 and 1556cm^{-1} were attributed to the formation of carbonyl and carboxyl groups in the adsorbents under study.

Table 4.4. Typical Absorption frequencies and Carbonyl stretching frequencies of Infra red spectra for free and metal loaded adsorbents

PSP-Cr^{3+}/Cr^{6+}	**APSP-Cr^{3+}/Cr^{6+}**	**SAPSP-Cr^{3+}/Cr^{6+}**	**PAPSP-Cr^{3+}/Cr^{6+}**	**9AAC-Cr^{3+}/Cr^{6+}**	**MPSP-Cr^{3+}/Cr^{6+}**	**Assignment**
3642/ 3438	3311/ 3618	3518/ 3615	3627/ 3601	-/-	3344/ 3463	-N-H, -O-H stretching
3016,2891/ 2886,2821	2913,2861/30 07,2886	3023,2894/30 88,2908	3076,2922/30 87,2895	2979,2880/29 86,2870	2914,2836/29 88,2885	-CH$_3$, -CH$_2$ symmetric stretch
2335/ 2347	2361/ 2347	2357/ 2356	2348/ 2355	2361/ 2356	2355/ 2359	Free CO$_2$
1722/ 1756, 1717	1719/ 1769, 1717	1776, 1711/ 1727	1707/ 1713	-/-	1752/ 1717	-C=O stretch for acids or aldehyde
1556/ 1589	1573/ 1573	1582/ 1573	1559/ 1571	1512/ 1573	1602/ 1589	-C=O& C=C Aromatic stretch for cellulose/ N-H bending of amide
1437/ 1487, 1435	1445/ 1496, 1435	1432/ 1444	1431/ 1430	1480,1435/ 1496, 1432	1451/ 1434	-CH$_2$- stretch/ -C=C- Aromatic stretching
1346/ 1354	1346/ 1355	1361/ 1367	1354/ 1349	1358/ 1342	1365/ 1345	-C-H stretch/ N-H bending
1291/ 1293, 1229	1242/ 1274, 1213	1260/ 1243	1277/ 1288, 1227	1292/ 1290, 1201	1258/ 1290, 1229	-C-O bending of carboxylic acids/ phenolic O-H stretch/ N-H bending
1224/ 1152	1126/ 1175	-/-	1221	1236	-/-	-O-H stretch (2^0 Alcohol), -C-O-C- stretching
1024/ 1063	1060/ 1046	1041/ 1045	1037/ 1060	1049/ 1060	1042/ 1062	-C-H stretch, -C-O stretch (1^0 Alcohol)
849/ 831	838/ 841	858/ 853	838/ 841	850/ 861	837/ 831	-C-H out of plane bending
785, 507/ 809, 512	798, 508/ 801, 501	718, 525/ 771, 519	786, 516/ 780, 520	793, 518/ 797, 503	801, 507/ 778, 526	Cr-O bending vibrations

The suppression of the peaks located at 1450-1750 cm^{-1} and the decrease of the ratio of the COOH and COO- groups intensities canbe observed. Also there is a shiftin the frequencies of the absorption band of both C=O and C-O in carboxyl group (-COOH) due to metal binding. The C-O band shifts to higher frequencies 1217-1289 cm^{-1}probably due to high electron density induced by the adsorption of chromium on the adjacent carbonyl groups [53, 54]. Thus carboxylic groups are involved in sorption of chromium as seen by comparison of IR spectra of the adsorbents and the chromium loaded-adsorbents. The interaction between chromium and carboxylic group of the adsorbent causes a diminution of the distance between C=O and C-O stretching peaks [55].A decrease in the ratio of the COOH and COO-groups intensities can also be observed. The carboxyl and carbonyl groups may further provide the binding sites for Cr^{3+} resulting from Cr^{6+} reduction. These observations suggest that Cr^{6+} induces an oxidation of lignincomponents which is not observed in Cr^{3+} loaded spectra and that the retention of Cr ions occurs througha complexation reaction involving carboxylate moieties. Similar observations were made by Dupont et al.[56].After Cr^{3+} adsorption intensity of the peak around 1630 cm^{-1} (C=O chelate stretching) increased.

4.3.6. X-Ray Photoelectron Spectroscopy.

Figure 4.9depicts the XPS spectra for the adsorbents under study after chromium adsorption. Table 4.5summarizes the identification of the bands observed in Figure4.9.

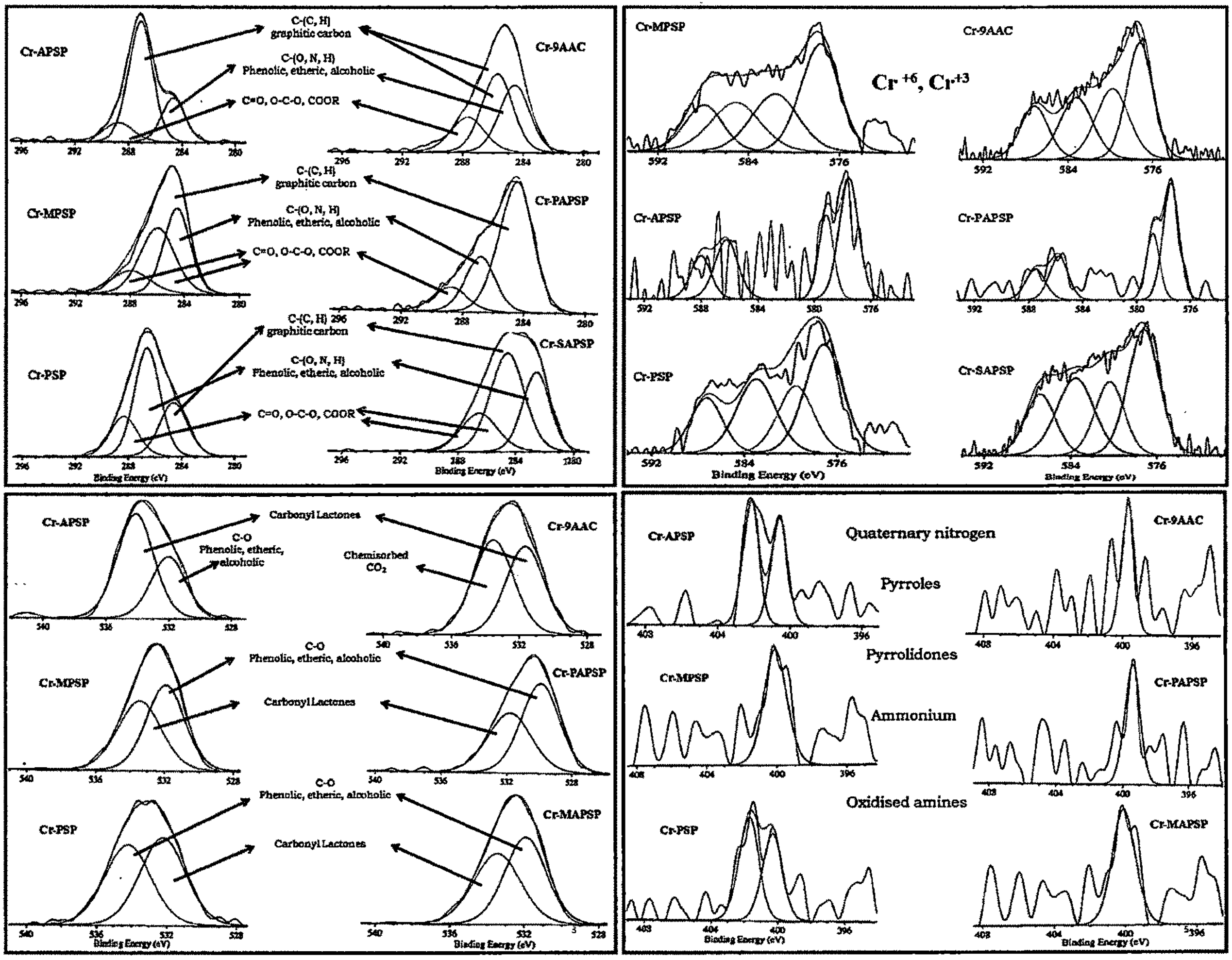

Figure 4.9. XPS spectra

It is also evident from the table that the five modified adsorbents of palm shell powder explored in this study have different amounts of carboxyl groups, differing by a factor up to 10. Furthermore, XPS results (Figure4.9 and Table 4.5) also showed an increase of carboxylate groups after Cr^{6+}adsorption.

Table 4.5. Summary of binding energy and area ratios of pristine and Cr-loaded adsorbents

Sample Surface	Proposed components	Binding Energy eV	FWHM eV	Relative Quantity %
C1s Valence State				
PSP	C-(C, H) graphitic C	284.661	2.310	0.6906
	C-(O, N, H) phenolic, alcoholic, etheric	285.984	1.774	0.1871
	C=O, O-C-O, COOR -carbonyl or quinine	287.200	2.495	0.1223
Cr-PSP	C-(C, H)	284.604	2.470	0.2820
	C-(OH, OR)	286.626	2.224	0.5119
	O=C-O carboxyl or ester	288.356	2.425	0.2061
APSP	C-(C, H)	284.647	2.462	0.6716
	C-(OH, OR)	286.599	2.074	0.2112
	O=C-O	288.577	2.605	0.1172
Cr-APSP	C-(C, H)	284.696	2.027	0.2219
	C-(OH, OR)	287.172	2.087	0.6459
	O=C-O	288.791	2.552	0.1239
SAPSP	C- (C, H)	284.524	2.264	0.5272
	C-(OH, OR)	286.342	1.894	0.2499
	O=C-O	288.073, 289.791	1.973, 2.181	0.1471, 0.0758
Cr-SAPSP	C-(C, H)	282.615	2.189	0.3139
	C-(C, H)	284.600	2.724	0.4839
	C-(OH, OR)	286.573	2.938	0.2019
PAPSP	C-(C, H)	284.590	2.051	0.6297
	C-(OH, OR)	286.071	2.204	0.2552
	C=O, O-C-O, COOR	287.979	1.527	0.0817
	O=C-O	289.308	1.424	0.0334
Cr-PAPSP	C-(C, H)	284.631	2.542	0.6439
	C-(OH, OR)	286.903	2.251	0.2379
	C=O, O-C-O, COOR, O=C-O	288.830	2.510	0.1179
9AAC	C-(C, H)	284.507	2.336	0.5552
	C-(OH, OR)	286.511	2.284	0.2822
	C=O, O-C-O, COOR	288.384	2.572	0.1155
	C=C, occluded CO, π electrons in aromatic ring, CO_2	290.295	3.464	0.0471
Cr-9AAC	C-(C, H)	284.607	2.325	0.3610
	C-(OH, OR)	285.755	2.352	0.1744
	C=O, O-C-O, COOR	287.709	2.360	0.0829
MPSP	C-(C, H, R), C-(C, H)	284.624	2.460	0.5456

	C-(OH, OR)	286.116, 286.346	1.718, 2.120	0.2137, 0.1311
	C=O, O-C-O, COOR O=C-O	288.517	2.491	0.1095
Cr-MPSP	C-(C, H, R), C-(C, H)	284.600	2.265	0.4149
	C-(OH, OR)	286.044	2.970	0.4189
	C=O, O-C-O COOR	287.993	3.355	0.1661
O1s Valence State				
PSP	C=O, C-O (Lactones, phenolic and etheric)	531.400	2.050	0.4424
	Singly bonded oxygen C-O	532.846	2.072	0.5576
Cr-PSP	C=O, C-O (Lactones, phenolic and etheric)	532.261	3.015	0.5219
	Singly bonded oxygen C-O	534.258	3.038	0.4819
APSP	C=O, C-O (Lactones, phenolic and etheric)	531.770	2.606	0.8160
	Singly bonded oxygen C-O	533.570	2.394	0.4796
Cr-APSP	C=O, C-O (Lactones, phenolic and etheric)	532.068	2.568	0.6411
	Singly bonded oxygen C-O	534.179	2.696	0.5067
SAPSP	C=O (Carboxylic acid)	532.209, 534.596	3.492, 3.517	0.8032, 0.1968
Cr-SAPSP	C=O, C-O (Carboxylic acid, etheric, lactonic, anhydrides, pyrones and phenols)	530.624, 532.541	2.964, 3.082	0.6129, 0.3871
PAPSP	C=O, C-O (Carboxylic acid, etheric, lactonic, anhydrides, pyrones and phenols)	531.656 533.388	2.449 3.347	0.4576 0.5424
Cr-PAPSP	C=O, C-O (Carboxylic acid, etheric, lactonic, anhydrides, pyrones and phenols)	529.984 531.841	2.771 3.095	0.5679 0.4320
9AAC	C=O, C-O (Carboxylic acid, etheric, lactonic, anhydrides, pyrones and phenols)	533.080	3.389	0.8437
	Occluded CO, chemisorbed CO_2, O_2 and H_2O	535.638	3.618	0.1563
Cr-9AAC	C=O, C-O (Carboxylic acid, etheric, lactonic, anhydrides, pyrones and phenols)	531.691 533.576	2.643 2.790	0.4701 0.5299
MPSP	C=O, C-O (Carboxylic acid, etheric, lactonic, anhydrides, pyrones and phenols)	531.367 532.931	2.440 2.978	0.3795 0.6205
Cr-MPSP	C=O, C-O (Carboxylic acid, etheric, lactonic, anhydrides, pyrones and phenols)	531.990 533.503	2.576 2.916	0.5219 0.4781
N1S				
PSP	C-N-C (pyrrolic nitrogen, pyridines)	399.839, 398.597,	1.492, 1.512,	0.6129, 0.2141,

		400.846	1.258	0.1729
Cr-PSP	C-N-C (pyrrolic nitrogen, pyridones)	400.382, 401.790	1.366, 1.368	0.4569, 0.5430
APSP	C-N-C (pyrrolic nitrogen, pyridones)	399.98, 400.075	1.228, 1.468	0.3556, 0.2780
	Quartenary nitrogen, protonated pyridinic ammonium ions, nitrogen atoms replacing carbon in graphene	401.278	1.908	0.3664
Cr-APSP	C-N-C (pyrrolic nitrogen, pyridones)	400.622	1.044	0.4709
	Oxidised nitrogen functionalities or NO_2 groups	402.245	1.000	0.5290
SAPSP	C-N-C (pyrrolic nitrogen, pyridones)	399.797	1.366	0.3883
	Quartenary nitrogen, protonated pyridinic ammonium ions, nitrogen atoms replacing carbon in graphene	401.477	1.941	0.6118
Cr-SAPSP	C-N-C (pyrrolic nitrogen, pyridones)	399.279	1.051	1.000
PAPSP	C-N-C (pyrrolic nitrogen, pyridones)	398.584, 399.774	1.097, 1.319	0.2677, 0.4869
	Quartenary nitrogen, protonated pyridinic ammonium ions, nitrogen atoms replacing carbon in graphene	401.074	1.032	0.2454
Cr-PAPSP	C-N-C (pyrrolic nitrogen, pyridones)	399.483	1.047	1.000
9AAC	C-N-C (pyrrolic nitrogen, pyridones)	397.686, 400.803	1.516, 1.596	0.3000, 0.3745
	Oxidised nitrogen functionalities or NO_2 groups	402.300	1.639	0.3255
Cr-9AAC	C-N-C (pyrrolic nitrogen, pyridones)	399.800	0.841	1.000
MPSP	C-N-C (pyrrolic nitrogen, pyridones)	398.703, 400.000	1.889, 1.679	0.2787, 0.5613
	Quartenary nitrogen, protonated pyridinic ammonium ions, nitrogen atoms replacing carbon in graphene	401.606	1.570	0.1599
Cr-MPSP	C-N-C (pyrrolic nitrogen, pyridones)	400.085	1.497	1.000

The presence of adsorbed chromium has been detected on the metal loaded adsorbents, and the Cr2p peaks have been analyzed. It consists of two contributions corresponding to 2p1/2 and 2p3/2 energy levels respectively as shown in table 4.6. The two contributions of Cr2p peaks are at 577.2,577.6,577.3, 577.5, 577.2, 577.8 eVand 587.2, 588.0,586.9,587.5, 587.2, 588.0eV for PSP,APSP,SAPSP, PAPSP, 9AAC and MPSP respectively. These values compare well with the binding energy of Cr^{3+}[56]. The slight difference between the Cr 2p1/2 peaks (586.8-587 eV) Cr2p3/2 peaks (577.2-577.7 eV) is attributed to different chemical environments. The Cr2p peaks which appear at 579.6, 579.2, 580.4,578.9,579.98, 581.7and 583.0, 586.2, 583.6, 585.8, 583.3, 585.2eV indicate the presence of hexavalent chromium and that reduction is not still complete. Similar observations were made by Dupont et al. [56].

Table 4.6. Summary of binding energy, area ratios, spin orbit splitting of Cr-loaded carbons

Sample Surface	Proposed components	Binding Energy eV	FWHM eV	Relative Quantity%	Spin orbit splitting
Cr-PSP	Cr2p 3/2 Cr^{3+}	577.210, 587.292	3.791, 3.193	0.3700, 0.1571	10.08
	Cr2p 1/2 Cr^{3+}	583.048	3.897	0.2579	
	Cr2p3/2 Cr^{6+}	579.596	3.582	0.2149	
Cr-APSP	Cr2p 3/2 Cr^{3+}	577.574, 588.019	1.590, 1.645	0.4059, 0.1480	10.5
	Cr2p 1/2 Cr^{3+}	586.227	1.872	0.2320	
	Cr2p3/2 Cr^{6+}	579.200	1.192	0.2129	
Cr-SAPSP	Cr2p 3/2 Cr^{3+}	577.246, 586.852	3.393, 3.268	0.3659, 0.1711	9.6
	Cr2p 1/2 Cr^{3+}	583.611	4.025	0.2659	
	Cr2p3/2 Cr^{6+}	580.424	3.146	0.1980	
Cr-PAPSP	Cr2p 3/2 Cr^{3+}	577.518, 587.514	1.357, 1.682	0.4469, 0.1461	10.0
	Cr2p 1/2 Cr^{3+}	585.803	1.590	0.1940	
	Cr2p3/2 Cr^{6+}	578.860	1.144	0.2130	
Cr-9AAC	Cr2p 3/2 Cr^{3+}	577.274, 587.224	2.843, 3.070	0.3419, 0.1671	10.0
	Cr2p 1/2 Cr^{3+}	583.290	3.601	0.2279	
	Cr2p3/2 Cr^{6+}	579.856	3.649	0.2630	
Cr-MPSP	Cr2p 3/2 Cr^{3+}	577.796, 588.053	3.931, 3.912	0.3739, 0.1591	10.3
	Cr2p 3/2 Cr^{6+}	581.715	4.875	0.2470	
	Cr2p1/2 Cr^{3+}	585.253	5.142	0.2210	

XPS results also showed the presence of Cr^{3+}(~40-50%) on Cr^{6+}loaded adsorbents. The carboxyl and carbonyl groups may further provide the binding sites for Cr^{3+}resulting from Cr^{6+}reduction. This is also supported by the fact that the adsorption capacity of all the adsorbents under study is greater for Cr^{6+} than Cr^{3+}. This observation is in agreement with the ICP analysis, which showed that almost no Cr^{3+} can be detected in the supernatants of the contacted solutions suggesting that the reduced Cr^{3+}is also strongly adsorbed at pH1 leading to maximum adsorption of total Cr at pH 1.Low pH also accelerates the redox reactions in aqueous and solid phases, since the protons participate in these reactions as Eq. (1).

$$HCrO_4^- + 7H^+ + 3e^- \leftrightarrow Cr^{3+} + 4H_2O \quad (1)$$

An increase in the O/C ratio is also observed from the XPS data which can be attributed to the conversion of *C*1 into *C*2 and*C*3 carbon types and generation of oxidized functional groups like alcoholic and carboxylic sites as also evidenced by IR spectral analysis. This interpretation is supported by thestudies of Pizzi[57] and Ostmeyer and Elder [58].

4.3.7. Column studies.

The column breakthrough curves for chromium adsorption by adsorbents under study are shown in Figure 4.10. The effluent concentration is seen to have the typical 'S' shape. A total of ~ 2.3 L of 1000 mg/L metal ion solution was passed through the column containing 5 g of adsorbent under study.Cr^{6+}adsorption in column mode showed adsorption upto155, 388, 375, 356, 164,162 bed volumes for PSP, APSP, SAPSP, PAPSP, 9AAC, MPSP respectively and 144, 347, 325, 335, 312, 131bed volumes for PSP, APSP, SAPSP, PAPSP, 9AAC and MPSP respectively for Cr^{3+}.

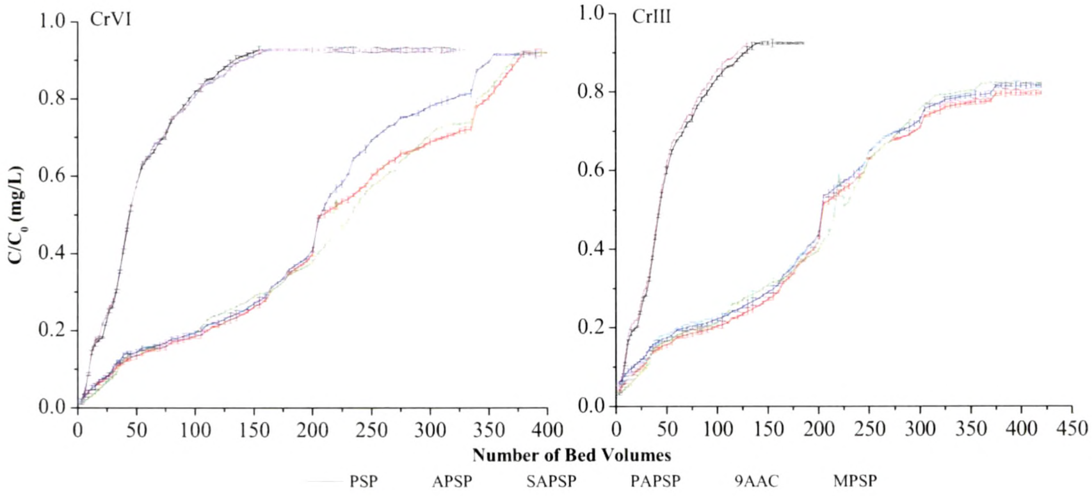

Figure 4.10. Column studies

Thomas and Yoon–Nelson models were also applied to the column adsorption data at a flow rate of 1 mL/min at an initial metal ion concentration of 1 g/L and bed height 5 cm with all the adsorbents under study.Thomas rate constant (k_{Th}) and bed capacity (q_{Th}) were calculated and are presented in Table 4.7.

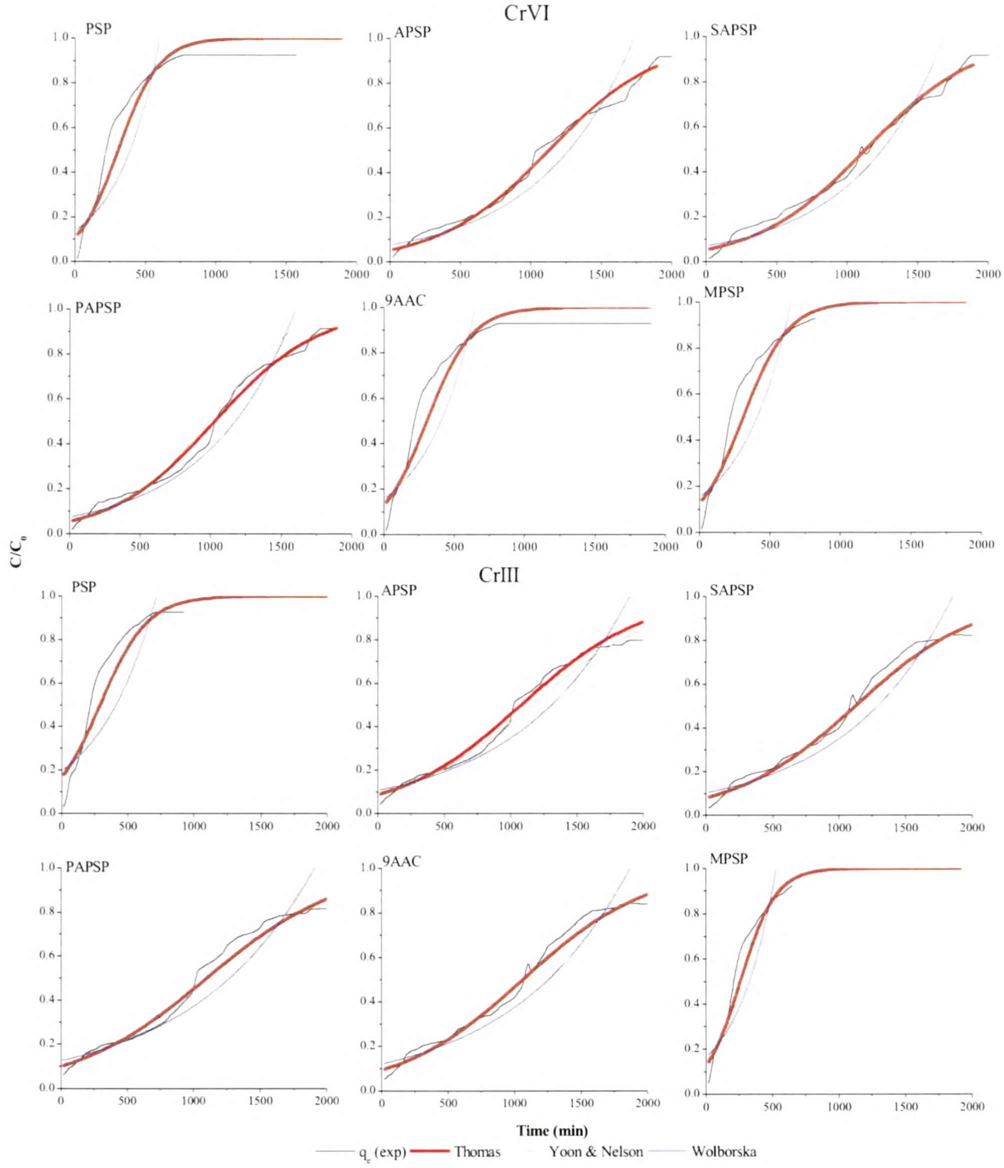

Figure 4.11. Column Modeling studies for Cr^{6+}& Cr^{3+}

The theoretical predictions based on the model parameters are compared in Figure 4.11 with the observed data. Similarly, from the plot of sampling time (t) versus $\ln[C_e/(C_0-C_e)]$, the Yoon and Nelson constant K_{YN} and τ (the time necessary to reach 50% of the retention) were calculated and are shown in Table 4.7. The well fit of the experimental data on to the Thomas and Yoon-Nelson model indicate that external and internal diffusion will not be the limiting step.

Table 4.7. Column Isotherms parameters for different adsorbents

Cr^{6+}/ Cr^{3+}	PSP	APSP	SAPSP	PAPSP	9AAC	MPSP
Thomas Model						
K_{TH}	0.000007/ 0.000006	0.000003/ 0.000002	0.000003/ 0.000002	0.000003/ 0.000002	0.000006/ 0.000002	0.000006/ 0.000008
q_0	61.739/ 58.097	225.910/ 216.514	226.406/ 224.771	206.349/ 220.310	61.312/ 213.084	62.080/ 51.531
r^2	0.937/ 0.938	0.986/ 0.982	0.976/ 0.980	0.984/ 0.985	0.938/ 0.985	0.935/ 0.969
SD	0.086/ 0.090	0.045/ 0.054	0.093/ 0.085	0.066/ 0.025	0.086/ 0.043	0.063/ 0.077
Yoon & Nelson Model						
K_{YN}	0.007/ 0.006	0.002/ 0.002	0.003/ 0.002	0.003/ 0.002	0.006/ 0.002	0.006/ 0.008
$t_{0.5(exp)}$	225/ 300	1050/ 1175	1100/ 1125	1050/ 1100	225/ 1075	225.000/ 250
$t_{0.5(cal)}$	309/ 291	1129/ 1157	1133/ 1124	1033/ 1102	307/ 1065	310/ 257
r^2	0.938/ 0.938	0.986/ 0.982	0.975/ 0.980	0.984/ 0.985	0.938/ 0.985	0.934/ 0.969
SD	0.086/ 0.090	0.091/ 0.054	0.096/ 0.085	0.066/ 0.025	0.086/ 0.043	0.064/ 0.077
Wolborska Model						
β	0.509/ 0.416	0.662/ 0.571	0.680/ 0.581	0.662/ 0.529	0.474/ 0.538	0.479/ 0.461
N_0	154424/ 182606	441653/ 483688	430902/ 472726	408938/ 486223	165709/ 476453	165752/ 134924
r^2	0.789/ 0.796	0.950/ 0.946	0.923/ 0.932	0.949/ 0.954	0.788/ 0.944	0.782/ 0.866
SD	0.062/ 0.096	0.082/ 0.060	0.077/ 0.091	0.089/ 0.023	0.067/ 0.057	0.084/ 0.093

From the equations in Chapter 3 Table3.1 it is evident that the characteristic parameter associated with Thomas and Yoon and Nelson models vary but both the models predict essentially same uptake capacity and C/C_0 values for a particular experimental set of data. Hence same r^2 and SD values were obtained as also suggested by Baral et al. [59].

4.3.8. Desorption.

The XPS results indicate that about 50% of Cr is present as Cr^{3+} and the rest as Cr^{6+}. As mentioned previously, ICP analysis was done to find the total Cr remaining in solution during the course of our adsorption studies. There was negligible difference in total chromium(obtained from ICP) and Cr^{6+}concentration(obtained from diphenylcarbazide method) due to the fact that Cr^{3+} was also retained almost quantitatively at pH1as indicated during pH studies. This led us to believe that complete reduction of $Cr^{6+}$to Cr^{3+} was taking place by the adsorbents under study as observed in many reports available in literature[60].Theanalysis thus not gives us a clue of only partial reduction Cr^{3+}.So no attempt was made to study the desorption of Cr as we felt that chromium present in the adsorbents under study need not be separated since the end product is a Cr^{3+} salt[61].

The partial reduction of $Cr^{6+}$to $Cr^{3+}$by the adsorbents under study was identified only from XPS studies, the results of which were unfortunately obtained only when we had almost come to an end of the compilation of this report. So further studies need to be done regarding desorption of Cr from the adsorbents under study and also to try to achieve complete reduction using a suitable desorbent as achieved by Luis K. [29].

4.4.Mechanism.

The aqueous phase pH governs the speciation of metals and also the dissociation of active functional sites on the sorbent. In this study, the pH values of initial solutions were adjusted to below 4.0 and the acidic chromate ion species ($HCrO_4^-$) was the major form of Cr^{6+} at this pH range [62]. At low pH conditions, there is easier protonation of functional groups such as amino, carboxyl and sulfonate groups of biomaterials making the adsorbent material surfaces more positive [63, 64].Furthermore, the point of zero charge (pH_{ZPC}) of the adsorbents under study was determined to be about in the range 3.5-4.0, suggesting that the adsorbents have a large surface charge density at pH 1, resulting in a strong electrostatic attraction between theadsorbents and the anionic adsorbates.

This results in the removal rate of Cr^{6+}in the aqueous phase being faster, since the binding of anionic Cr^{6+}species with the positively charged groups is enhanced as a result of electrostatic interaction.Thus, Cr^{6+}sorption, similar to other metals, could easily be attributed to ion exchange, surfacecomplexation, and precipitation.The reason being reduction of $Cr^{6+}$to Cr^{3+}could not be evidenced by the presence of Cr^{3+} in solution as observed by other researchers. However, low pH is also known to accelerate the redox reactions in aqueous and solid phases, since the protons participate in these reactions as[65].The chromium reduction can take place through variousreactions, mainly the following;

$$CrO_4^{2-} + 8H^+ + 3e^- \leftrightarrow Cr^{3+} + 4H_2O \qquad E^0=1.48\ V$$

$$HCrO_4^- + 7H^+ + 3e^- \leftrightarrow Cr^{3+} + 4H_2O \qquad E^0=1.35\ V$$

$$H_2CrO_4 + 6H^+ + 3e^- \leftrightarrow Cr^{3+} + 4H_2O \qquad E^0=1.33V$$

The electron donor groups of the biomass reduce $Cr^{6+}$to Cr^{3+}. After that, Cr^{3+}forms complexes with the adsorbent materials under study.Furthermore,XPS analyses suggested the presence of both $Cr^{3+}$and Cr^{6+} species on the adsorbent surfaces. This suggests that Cr^{6+} anions were easily adsorbed on the adsorbents by electrostatic interaction and were reduced to Cr^{3+} ions on the biomass surface.The adsorption of $Cr^{3+}$was also found to be quantitative at low pH probably due to chelation of $Cr^{3+}$with hydroxyl and phenolic groups. After reduction, either $Cr^{3+}$was occluded in the solid phase or slow to diffuse back to aqueous phase that Cr^{3+} was undetectable in the filterate.FT-IR observations also suggest that hexavalent Cr induces an oxidation of lignin components and that the retention of Cr ions occurs through a complexation reaction involving carboxylate moieties.

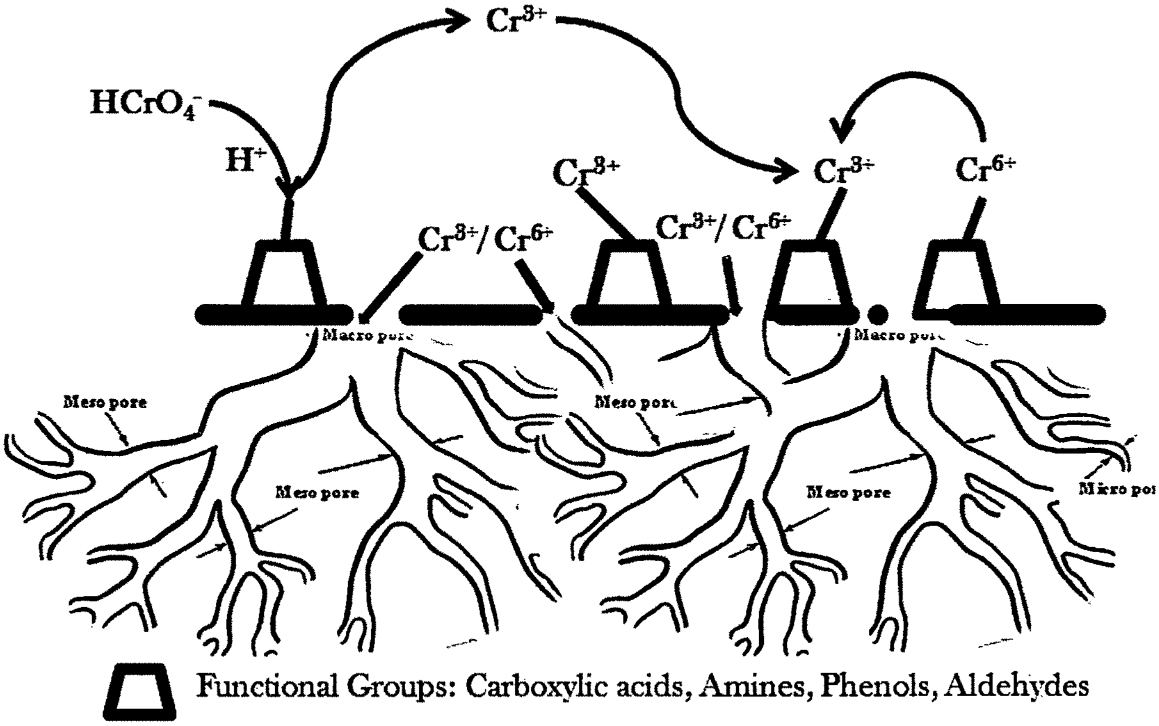

Figure 4.12. Mechanism for Cr^{6+} and Cr^{3+} adsorption and reduction of chromium involved

The adsorption process thus probably involves three steps as depicted in Figure 4.12: (1) the binding of anionic Cr^{6+} ions with the positively charged groups present on the biomass surface; (2) the reductionof Cr^{6+} to Cr^{3+} by adjacent electron-donor groups; (3) the formation of complexes of the Cr^{3+} with adjacent groups capable of Cr-binding. This statement was consistent withthat of Park et al. [66-68].

Literature Cited:

1. V.P. Evangelou, *Environmental Soil and Water Chemistry: Principles and Applications*; John Wiley&Sons: NewYork, **1998**; 476.
2. R. Eisler, *Chromium Hazards to Fish, Wildlife, and Invertebrates: A Synoptic Review*; Biological Report 85 1.6; Contaminated Hazard Reviews Report 6; U.S. Department of the Interior, Fish and Wildlife Service: Laurel, MD, **1986**.
3. S.D. Faust, O. M. Aly, *In Adsorption Processes of Water Treatment*; Butterworth Publishers: Stoneham, MA, **1987**.
4. C. Raji, T. S.Anirudhan.*Water Res.* **1998**, *32*, 3772.
5. L.J. Yu, S.S. Shukla, K.L. Dorris, A. Shukla, J.L. Margrave. *J. Hazard. Mater.* **2003**, *100*, 53.
6. F.N. Acar, E. Malkoc.*Bioresource Technol.* **2004**, *94*, 13.
7. H. Ucun, Y.K. Bayhan, Y. Kaya, A. Cakici, O.F. Algur.*Bioresource Technol.* **2002**, *85*, 155.
8. J.S. Melo, S.F. D'Souza.*Bioresource Technol.* **2004**, *92*, 151.
9. R.S. Bai, T.E. Abraham.*J. Sci. Ind. Res.* **1998**, *57*, 821.
10. J.S. Merrin, R. Sheela, N. Saswathi, R.S. Prakasham, S. V.Ramakrishma.*Indian J. Exp. Biol.* **1998**, *36*, 1052.
11. R.S. Prakasham, J.S. Merrie, R. Sheela, N. Saswathi, S.V. Ramakrishna. *Environ. Pollut.***1999**, *104*, 421.
12. Y. Sag, A. Yalcüuk, T. Kutsal.*Hydrometallurgy*.**2001**, *59*, 77.
13. M. Nourbakhsh, Y. Sag, D. Ozer, Z. Aksu, T. Kutsal, A.A. Cuaglar.*Process Biochem.* **1994**, *29*, 1.
14. G. Ozdemir, T. Ozturk, N. Ceyhan, R. Isler, T. Cosar.*Bioresource Technol.* **2003**, *90*, 71.
15. A.I. Zouboulis, M.X. Loukidou, K.A. Matis.*Process Biochem.* **2004**, *39*, 909.
16. Z. Aksu,U. Acüikel, T. Kutal. *J. Chem. Technol. Biotechnol.* **1997**, *70*, 368.
17. G.C. Donmez, Z. Aksu, A. Ozturk, T. Kutsal.*Process Biochem.* **1999**, *34*, 885.
18. Z. Aksu, U. Acüikel.*Biochem. Eng. J.* **2000**, *4*, 229.
19. V.K. Gupta, A.K. Shrivastava, N. Jain.*Water Res.* **2001**, *35*, 4079.
20. D.C. Lee, C.J. Park, J.E. Yang, Y.H. Jeong, H.I. Rhee.*Appl. Microbiol. Biotechnol.* **2000**, *54*, 445.
21. D. Park, Y.S. Yun, J.M. Park.*Environ. Sci. Technol.***2004**, 38, 4860.
22. L. Chun, C. Hongzhang, L. Zuohu.*Process Biochem.* **2004**, *39*, 541.
23. N.R. Bishnoi, M. Bajaj, N. Sharma, A. Gupta.*Bioresource Technol.* **2004**, *91*, 305.
24. K. Selvaraj, S. Manonmani, S. Pattabhi.*Bioresource Technol.* **2003**, *89*, 207.

25. D. Mohan, C. Pittman.*J. Hazard. Mater.* **2006**,*B137*, 762.
26. C. Raji, T.S. Anirudhan.*Indian J. Chem. Technol.* **1997**, *4*, 228.
27. M. Zhao, J.R. Duncan.*Biotechnol. Appl. Biochem.* **1997**, *26*, 179.
28. D. Kratochvil, P. Pimentel, B. Volesky.*Environ. Sci. Technol.* **1998**, *32*, 2693.
29. L.K. Cabatingan, R.C. Agapay, J.L. Rakels, M. Ottens, L.A.M. Van der Wielen.*Ind. Eng. Chem. Res.* **2001**, *40*, 2302.
30. D.C. Sharma, C.F. Forster.*Water Res.* **1993**, *27*, 1201.
31. J.L. Gardea-Torresdey, K.J. Tiemann, V. Armendariz, L. Bess-Oberto, R.R. Chianelli, J. Rios, J.G. Parsons, G. Gamez.*J. Hazard. Mater.* **2000**, *80*, 175.
32. In-situ treatment of soil and groundwater con-taminated with chromium, Technical Resources Guide, United States Environmental Protection Agency, US EPA/625/R-00/005.
33. Dionex, Determination of Cr(VI) in water, wastewater and solid waste extracts,Technical Note 26LPN34398-011M7/96, Dionex Corporation, **1996**.
34. V.M. Nurchi, G. Crisponi, I. Villaescusa. *CoordChem Rev.***2010**, *254*, 2181.
35. R. Ramos, A. Martinez, R. Coronado.*Water Sci. Technol.***1994**, *30*, 19.
36. M. Lopez-Garcia, P. Lodeiro, J.L. Barriada, R. Herrero, M.E. Sastre de Vicente. *Chem. Eng. J.* **2010**, *165*, 517.
37. S.K. Das, A.R. Das, A.K. Guha. *Environ. Sci. Technol.* **2007**, *41*, 8281.
38. B. Xiao, K.M. Thomas. *Langmuir* **2005**, *21*, 3892.
39. J. Febrianto, A.N. Kosasih, J. Sunarso, Y.H. Ju, N. Indraswati, S. Ismadji. *J. Hazard. Mater.* **2009**, 162.
40. R.S. Vieira, M.M. Beppu. *Colloids Surf. A.***2006**, *279*, 196.
41. Y.S. Ho, G. McKay. *Chem. Eng. J.* **1998**, *70*, 115.
42. S. Schiewer, S.B. Patil. *Biores. Technol.* **2008**, *99*, 1896.
43. Z. Reddad, C. Gerente, Y. Andres, P.L. Cloirec. *Environ. Sci. Technol.* **2002**, *36*, 2067.
44. K. Vijayaraghavan, K. Palanivelu, M. Velan. *Biores. Technol.* **2006**, *97*, 1411.
45. J. Sarma, A. Sarma, K.G. Bhattacharyya. *Ind. Engg. Chem. Res.***2008**, *47*, 5433.
46. V.K. Gupta, I. Ali, V.K. Saini, T.V. Gerven, B.V. Bruggen, C. Vandecasteele. *Ind. Eng. Chem. Res.***2005**, *44*, 3655.
47. G.J.L. Torresdey, K. Dokken, K.J. Tiemann, J.G. Parsons, J. Ramos, N.E. Pingitore, G. Gamez. *Microchem. J.* **2002**, *71*, 157.
48. R.K. Samal, B.B. Panda, S.K. Rout, M. Mohanty.*J. Appl. Polym. Sci.* **1995**, *58*, 745.
49. K.K. Pandey.*J. Appl. Polym. Sci.* **1999**, *71*, 1969.
50. H. Yang, R. Yan, H. Chen, D.H. Lee, C. Zheng.*Fuel.***2007**, *86*, 1781.

51. M.S. Elovitz, W. Fish.*Environ. Sci. Technol.* **1995**, *29*, 1933.

52. A. Santos, P. Yustos, A. Quintanilla, S. Rodriguez, F. Garcia-Ochoa.*Appl. Catal.B.* **2002,** *39*, 97.

53. E. Fourest, B. Volesky. *Environ. Sci. Technol.* **1996**, *30*, 277.

54. N.B. Clothup, L.H. Daly, S.E. Wiberley. *Introduction to Infrared and Raman Spectroscopy, 3rd ed.*; Academic Press: London, **1990**.

55. S. Fonglim, Y. Mingzheng, S. Wenzou, J.P. Chen. *Environ. Sci. Technol.* **2008**, *42*, 2551.

56. L.Dupont, E.Guillon. *Environ. Sci. Technol.* **2003**, *37*, 4235.

57. A. Pizzi, *Holzforschung***1990**, *44*, 419.

58. J. G.Ostmeyer, T. J. Elder, *J. Wood Technol.* **1988**, 8, 413.

59. S.S. Baral, N. Das, T.S. Ramulu, S.K. Sahoo, S.N. Das, G.R. Chaudhury. *J. Hazard. Mater.***2009,** *161*, 1427.

60. J. Li, Q. Lin, X. Zhang, Y. Yan.*J. Colloid Interface Sci.* **2009,***333*, 71.

61. R. Aravindhan, B. Madhan, J.R. Rao. *Environ. Sci. Technol.***2004**, *38*, 300.

62. R. Ramos, A. Martinez, R. Coronado, *Water Sci. Technol.* **1994,** *30*, 191.

63. D.C. Sharma, C.F. Forster, *Bioresour. Technol.* **1994**, *47*, 257.

64. G. Cimino, A. Passerini, G. Toscano, *Water Res.* **2000,** *34*, 2955.

65. D. Park, S.R. Lim, Y.S. Yun, J.M. Park, *Bioresour. Technol.* **2008**, *99*, 8810.

66. D. Park, Y.S. Yun, J.M. Park, *Environ. Sci. Technol.* **2004**, *38*, 4860.

67. D. Park, Y.S. Yun, J.M. Park, *Chemosphere.***2005**, *60*, 1356.

68. D. Park, Y.S. Yun, D.S. Lee, S.-R. Lim, J.M. Park, *J. Hazard. Mater.* **2006,** *137*, 1377.